

First Results from the Heidelberg Dark Matter Search Experiment

L. Baudis ^{*}, A. Dietz, B. Majorovits, F. Schwamm, H. Strecker and H. V. Klapdor-Kleingrothaus [†]
Max-Planck-Institut für Kernphysik, Heidelberg, Germany

The Heidelberg Dark Matter Search Experiment (HDMS) is a new ionization Germanium experiment in a special design. Two concentric Ge crystals are housed by one cryostat system, the outer detector acting as an effective shield against multiple scattered photons for the inner crystal, which is the actual dark matter target. We present first results after successfully running the prototype detector for a period of about 15 months in the Gran Sasso Underground Laboratory. We analyze the results in terms of limits on WIMP-nucleon cross sections and present the status of the full scale experiment, which will be installed in Gran Sasso in the course of this year.

I. INTRODUCTION

Weakly Interacting Massive Particles (WIMPs) are leading candidates for the dominant form of matter in our Galaxy. These hypothetical, relic particles from an early phase of the Universe are predicted independently from cosmological considerations by supersymmetric particle physics theories as neutralinos - the lightest supersymmetric particles.

Direct WIMP detection experiments exploit the elastic WIMP scattering off nuclei in a terrestrial detector [1]. However, detecting WIMPs is not a simple task. As their name suggests, their interaction with matter is very feeble ($\sigma \leq \sigma_{weak}$) and predicted rates in supersymmetric models range from 10 to 10^{-5} events per kilogram of detector material and day [2]. Moreover, for WIMP masses between a few GeV and 1 TeV, the energy deposited by the recoil nucleus is less than 100 keV. Thus, in order to be able to detect a WIMP, an experiment with a low energy threshold and an extremely low radioactive background is required. Since the reward would be no less than discovering the dark matter in the Universe, a huge effort is put into direct detection experiments. More than a dozen of experiments are running at present and even more are planned for the future (for recent reviews see [3,4,5]).

The focus of this paper is to present first results of the Heidelberg Dark Matter Search (HDMS) prototype [6], which took data over a period of about 15 months in the Gran Sasso Underground Laboratory (LNGS) in Italy. After a description of the experimental setup, its performance is discussed in some detail. The last 49 days of data taking are analyzed in terms of WIMP-nucleon cross sections and a comparison to other running dark matter experiments is made. The status and the prospects of the full scale experiment are discussed and finally conclusions and an outlook are given.

II. DESCRIPTION OF THE EXPERIMENT

HDMS operates two ionization HPGe detectors in a unique configuration [6]. A small, p-type Ge crystal is surrounded by a well-type Ge crystal, both being mounted into a common cryostat system (see Figure 1 for a schematic view). To shield leakage currents on the surfaces, a 1 mm thin insulator made from vespel is placed between them. Two effects are expected to reduce the background of the inner, WIMP target detector with respect to our best measurements of the Heidelberg-Moscow experiment [7]. First, the anticoincidence between the two detectors acts as an effective suppression for multiple scattered photons, second, the detection crystal is surrounded by Ge, which is one of the radio-purest known materials. From previous measurements we know that the main radioactive background of Ge detectors comes from materials situated in the immediate vicinity of the crystals, i.e. from the copper parts of the cryostats [8].

In order to house both Ge crystals, a special design of the copper crystal holder system was required. The idea was to construct a pyramidal structure made of copper on top of the crystals, allowing to establish the two HV and two signal contacts, which are fixed by springs made from vespel (see Figure 2) [9]. In the prototype version three of the four contacts were unfortunately soldered by the manufacturer. The cryostat system was fabricated in Heidelberg from low radioactivity, electropolished copper. The FETs are placed 20 cm away from the crystals so that their effect

^{*}laura.baudis@mpi-hd.mpg.de

[†]klapdor@daniel.mpi-hd.mpg.de

on the background is minimized by a small solid angle and by 10 cm of copper shielding. For the prototype experiment both inner and outer detector are made of natural high-purity Germanium.

The data acquisition system of the HDMS experiment allows data sampling either in a calibration mode (filling a histogram in a memory module, fast data acquisition) or in an event-by-event mode where in addition the pulse-shape of an individual event can be recorded. The energy outputs of the preamplifiers are divided and amplified with two different shaping time constants ($3\ \mu\text{s}$ and $4\ \mu\text{s}$) and different gains at the spectroscopy amplifiers in order to record low energy (from threshold to 400 keV) and high energy (from 70 keV to 8 MeV) spectra. The spectra are measured with 13bit ADCs, which also release the trigger for an event by a peak detect signal. Further triggers are vetoed until the complete event information (arrival time with an accuracy of $100\ \mu\text{s}$, energy and eventually the pulse shape) has been recorded. The dead-time of $200\ \mu\text{s}$ (without pulse shape) is negligible for a typical event rate of 1.4×10^{-3} Hz in the outer detector. The anticoincidence between the two detectors is performed off-line.

III. DETECTOR PERFORMANCE IN HEIDELBERG

First tests of detector performance were done in the Heidelberg low level laboratory using standard calibration sources like ^{133}Ba , ^{60}Co , ^{214}Am and ^{152}Eu - ^{228}Th . The sensitivity of the detectors in their geometrical arrangement was tested by a scan measurement with a collimated ^{133}Ba source. The achieved energy resolutions and thresholds are shown in Table I along with other detector properties.

The concentric configuration of the two Ge-crystals gives rise to cross-talk events [10,11]. Using ^{133}Ba and ^{228}Th calibration sources, we recorded data in an event-by-event mode, to obtain two-dimensional scatter plots of deposited energies in each detector. These plots clearly visualize a linear correlation between energies in the inner and outer crystal, although in different strengths (see Figure 3).

The linear correlation between the energy depositions in the two crystals is corrected off-line. If E_i and E_o are the true ionization energies deposited in the inner and outer detector and E'_i , E'_o the measured energies, then one can write:

$$E_i = \frac{E'_i - k_{io} \times E'_o}{1 - k_{io} \times k_{oi}}, \quad E_o = \frac{E'_o - k_{oi} \times E'_i}{1 - k_{io} \times k_{oi}},$$

where k_{oi} and k_{io} are the slopes of the correlation lines. The width of the correlation lines is determined by the energy resolution of the detectors. The slopes are determined to be:

$$k_{io} = 0.00375 \pm 0.43 \times 10^{-4}$$

$$k_{oi} = 0.12850 \pm 0.27 \times 10^{-3}$$

The error in the energy determination arising from the cross-talk correction is a function of the error of the measured energy deposition and of the magnitude as well as the error of the slopes of the correlation lines. It can be inferred directly by comparing the widths of energy peaks in the two detectors after the cross-talk correction (for peaks with simultaneous energy deposition in the other detector, e.g. 511 keV or the ^{60}Co lines) with the widths of the same peaks for energy depositions in a single detector only. While for the inner detector the effect is negligible (note that k_{io} is much smaller than k_{oi}), for the outer detector the energy resolution worsens by 0.3% to 0.4% at 1332 keV. As we will see later, this has no influence on the anticoincidence spectrum between the two detectors. The cross-talk correction requires the stability of the slopes of the linear correlations. This stability has been monitored and confirmed. Another possibility to remove the cross-talk would be to introduce an extra grounded shield between the detectors. We refrained from applying this hardware solution because of strongly reduced Anti-Compton capability and the additional contamination risk.

IV. DETECTOR PERFORMANCE AT LNGS

The HDMS prototype was installed at LNGS in March 1998 and successfully took data over a period of about 15 month, until July 1999 [12]. Figure 4 shows the detector in its open shield. The inner shield is made of 10 cm of electrolytic copper, the outer one of 20 cm of Boliden lead, both lead and copper having been stored for several years below ground at Gran Sasso. The whole setup is enclosed in an air tight steel box and flushed with gaseous nitrogen in order to suppress environmental radon diffusion. Finally a 15 cm thick borated polyethylene shield surrounds the steel box to minimize the influence of neutrons.

The individual runs were about 0.9 d long. The experiment was stopped daily and parameters such as leakage currents of the detectors, nitrogen flow, overall trigger rate and count rate of the individual detectors were checked.

Energy calibrations were done weekly with standard ^{133}Ba and ^{152}Eu - ^{228}Th sources, introduced through a Teflon tube. The energy resolution of both detectors (1.2 keV at 300 keV inner detector and 3.2 keV at 300 keV outer detector) were stable as a function of time. The zero energy resolutions, which are determined by extrapolating the full widths at half maximum (FWHM) to 0 keV, are (1.06 ± 0.3) keV and (3.04 ± 0.3) keV for the inner and outer detector, respectively. Another way to specify the zero energy resolution is given by the cross talk correction. The cross talk generates ‘fake’ events beyond the energy thresholds of both detectors, which are then shifted to 0 keV by the correction. This allows a direct measurement of the energy resolution at 0 keV (see Fig. 5) and a cross check of the quality of the cross-talk correction at the same time. The values of 0.94 keV and 3.34 keV are fully consistent with the ones obtained by the FWHM-extrapolation.

To determine the energy threshold, a reliable energy calibration at low energies is required. The lowest-energetic lines observed in the detectors in the calibration mode were the ^{133}Ba line at 81 keV in the inner detector and the 121.8 keV line of ^{152}Eu in the outer one (all lower energetic lines are absorbed in the copper of the crystal holder system). However, intrinsic radioactivity of the crystals and/or of the surrounding copper such as the 10.37 keV line of ^{68}Ge and the 46.5 keV line of ^{210}Pb allowed to check the calibration down to low energies. The energy thresholds are 2.0 keV and 7.5 keV for the inner and outer detector, respectively.

After correction for the cross talk and re-calibration to standard calibration values (according to the weekly determined calibration parameters), the spectra of the daily runs were summed up. Figures 6 and 7 show the sum spectra for the outer and inner detector, respectively. The most important identified lines are labeled.

In the outer detector the lines of the cosmogenic isotopes ^{68}Ge , ^{57}Co , ^{58}Co , ^{54}Mn , ^{60}Co , ^{65}Zn , of the natural decay chains ^{238}U and ^{232}Th , of the primordial ^{40}K , of the anthropogenic radionuclide ^{137}Cs and the annihilation line at 511 keV can be identified. The statistics in the inner detector is lower, however the following lines can be clearly seen: ^{68}Ga K_β at 10.37 keV, ^{210}Pb at 46.5 keV, external ^{57}Co at 122.1 keV and internal at 143.6 keV (+ X-ray), 511 keV annihilation, ^{54}Mn at 834 keV, ^{60}Co at 1173 keV and 1332 keV and ^{40}K at 1460 keV. The region below 10 keV is dominated by the X-rays of ^{49}Ti (5 keV) and ^{55}Mn (6.5 keV). In addition to the outer detector, a structure centered at 32 keV with a FWHM of 2 keV is identified. Its origin is not yet fully understood, but could be a ^{210}Pb contamination at the inner contact with incomplete charge collection. Figure 8 shows the energy depositions in the inner detector as a function of measuring time. No microphonic events (bursts) can be seen beyond 2.0 keV. The decreasing activity of ^{68}Ge is nicely visualized.

After 363 days of pure measuring time the statistics in the inner detector was high enough in order to estimate the background reduction through the anticoincidence with the outer detector. In order to obtain true anticoincidence spectra, the energy thresholds for computing the anticoincidence must lie at least 3σ away from zero, where $\text{FWHM}_0=2.35\sigma$ is the zero energy resolution. Table II gives the energy thresholds and the zero energy resolutions for both detectors, after the cross talk correction. The energy thresholds lie in both cases about 5σ away from zero, so they count as cuts for computing the anticoincidence between the crystals. Thus, the fact that the zero energy resolution of the outer detector is worsened by the cross-talk correction does not affect the anticoincidence spectra between the two detectors.

Figure 9 shows the low-energy spectrum of the inner detector before and after the anticoincidence. The anticoincidence has no influence on the cosmogenic X-rays below 11 keV, as well as on the structure at 32 keV. The β^- spectrum from the cosmogenically produced ^3H with endpoint at 18 keV is most likely present as well. If the Compton suppression is applied in the energy region between 40 keV and 100 keV, the background reduction factor is 4.3. The counting rate after the anticoincidence in this energy region is 0.07 events/kg d keV, thus very close to the value obtained in the Heidelberg-Moscow experiment with the enriched detector ANG2 [7]. In the energy region between 11 keV and 40 keV the background index is a factor of 3 higher (0.2 events/kg d keV).

V. DARK MATTER LIMITS

The evaluation for dark matter limits on the WIMP–nucleon cross section $\sigma_{\text{scalar}}^{\text{W-N}}$ follows the method described in [7]. Because the cosmogenic radionuclides produced in the Ge crystals and in the surrounding copper have typical half-lives of 300 days, we consider only the last 49 d of measurement of the HDMS prototype. The total exposure corresponds to 9.9 kg d. The number of counts per 1 keV energy bin are listed in Table III. The background index in the energy region between 2–30 keV is 0.5 events/kg d keV. No background subtractions were applied. The parameters used in the calculation of expected WIMP spectra are given in Table IV.

The resulting upper limit exclusion plot in the $\sigma_{\text{scalar}}^{\text{W-N}}$ versus M_{WIMP} plane is shown in Fig. 10. At this stage, the limit is not yet competitive with our limit from the Heidelberg-Moscow experiment for large WIMP masses. However,

the cross section limits for WIMP masses below 40 GeV are considerably improved. This is mainly due to the lower energy threshold of 2 keV, compared to 9 keV in the Heidelberg-Moscow experiment. Also shown in the figure are limits from the Heidelberg-Moscow experiment [7], the Neuchâtel-experiment [18], the DAMA experiment [19] and the most recent limits from the CDMS experiment [20]. The filled contour represents the 2σ evidence region of the DAMA experiment [23]. The dashed line is the expectation for HDMS having a background index equal to the one of the Heidelberg-Moscow experiment [7] extended down to an energy threshold of 2 keV. The experimental limits are compared to expectations (scatter plot) for WIMP-neutralinos calculated in the MSSM parameter space at the weak scale (without any GUT constraints) under the assumption that all superpartner masses are lower than 300 GeV - 400 GeV [24].

VI. THE FULL SCALE HDMS EXPERIMENT

For the second phase of HDMS, important changes were already made. First, the inner crystal made of natural Germanium was replaced by an enriched ^{73}Ge crystal. In this way, we will be sensitive also to spin-dependent WIMP-nucleon interactions, since ^{73}Ge is the only Germanium isotope with spin. In addition, the ^{70}Ge isotope, which is the source of ^{68}Ge by the $^{70}\text{Ge}(p,t)^{68}\text{Ge}$ reaction, is now strongly depleted. Although the exact depletion is not measured yet, we expect at least a factor of 50 (we measured a factor of 60 depletion in ^{70}Ge for the enriched ^{76}Ge detectors in the Heidelberg-Moscow experiment [25]).

Second, the copper crystal holder system was replaced by a holder made of extremely radio-pure copper; soldering of the signal and the high-voltage contacts was not applied. We believe that both facts will have a large impact on the background of the HDMS detectors, since Monte Carlo simulations based on GEANT3.21 showed [26], that besides the cosmogenic activation of the crystals, the U/Th contamination of the copper and solder were the main background sources of the prototype.

The ^{73}Ge -HDMS detector has been assembled and transported by ship to Heidelberg, where its performance was tested in the low-level laboratory. Both inner and outer detector are working well, the (not optimized) energy resolutions being around 1.9 keV and 4.0 keV at 1332 keV. We will install the full scale experiment at LNGS in August 2000.

VII. SUMMARY AND OUTLOOK

The prototype detector of the HDMS experiment successfully took data at LNGS over a period of about 15 months. Most of the dominant background sources were identified. However, the origin of a structure centred at 32 keV in the inner detector is still unclear. Due to its low energy and the fact that it is not removed by the anticoincidence with the outer detector, it is most probably located in the inner crystal itself or at the signal contact. The future measurement with the ^{73}Ge -HDMS detector will hopefully help to clarify its nature.

The background reduction factor through anticoincidence in the inner detector in the energy region 40–100 keV is 4.3. It is less than previously expected [6], due to the smaller diameter of the outer, veto Ge-detector than originally planned. Nevertheless, the background in the energy region between 40 keV and 100 keV of the inner detector is with 0.07 events/kg d keV already now at the level of the Heidelberg-Moscow experiment. In the region between 2–30 keV it is with 0.5 events/kg d keV a factor of 7 higher, mainly due to the cosmogenic activation of the natural Ge crystals. However, due to the smaller energy threshold of 2 keV, the limits on WIMP-nucleon cross sections were improved for WIMP masses below 40 GeV with respect to the Heidelberg-Moscow experiment. They are currently the most stringent spin-independent limits at low WIMP masses for using raw data without any background subtraction.

The expectation for the ^{73}Ge -HDMS detector is shown in Fig. 10. It is based on a background index of 0.07 events/kg d keV in the region between 2–30 keV. The aim of HDMS is to test the ‘evidence region’ singled out by the DAMA experiment [23] in the MSSM parameter space after about two years of measurement. It would be an independent test by using only raw data and a completely different detection technique.

ACKNOWLEDGMENTS

We would like to thank Dr. Gerd Heusser and Dr. Yorck Ramachers for valuable discussions.

- [1] M. W. Goodman and E. Witten, Phys. Rev. D 31 (1985) 3059
- [2] G. Jungmann, M. Kamionkowski, K. Griest, Phys. Rep. 267 (1996) 195, V. Bednyakov, H.V. Klapdor-Kleingrothaus, S.G. Kovalenko, Y. Ramachers, Z. Phys. A 357 (1997) 339, Bottino et al., hep-ph/0001309
- [3] A. Morales, astro-ph/9912554 and in Proc. of the 6th Int. Workshop “TAUP99”, Paris, France 6-10 sept. 1999, Nucl. Phys. (Proc. Suppl.)
- [4] Y. Ramachers, astro-ph/9911260 and in Proc. XIth Rencontres de Blois, Frontiers of Matter, France, June 27 - July 3, 1999
- [5] L. Baudis, H.V. Klapdor-Kleingrothaus, astro-ph/0003434 and in Proceedings of Beyond the Desert '99, Second International Conference on Physics beyond the Standard Model, Castle Ringberg, Tegernsee, Germany, 6-12 June 1999, eds. H.V. Klapdor-Kleingrothaus, I.V. Krivosheina (IOP Bristol, 2000)
- [6] L. Baudis J. Hellmig, H.V. Klapdor-Kleingrothaus, A. Müller, F. Petry, Y. Ramachers, H.Strecker, Nucl. Instrum. Methods A 385, 265 (1997)
- [7] L. Baudis et al., (Heidelberg-Moscow collaboration), Phys. Rev. D 59 (1998) 022001-1
- [8] H.V. Klapdor-Kleingrothaus et al., (Heidelberg-Moscow collaboration), submitted to Phys. Lett. B
- [9] The layout was designed by Greg Martin, EG&G Ortec, Oak Ridge, Tennessee
- [10] Y. Ramachers, Dissertation, University of Heidelberg, 1997
- [11] L. Baudis et al., Nucl. Phys. B (Proc. Suppl.) 70 (1999) 106
- [12] L. Baudis, Dissertation, University of Heidelberg, 1999
- [13] R. Bernabei, Riv. Nuovo Cimento 18, (1995) 1
- [14] J.D. Lewin and P.F. Smith, Astropart. Phys. 6, 87 (1997).
- [15] K. Freese, J. Frieman, and A. Gould, Phys. Rev. D 37, 3388 (1988).
- [16] P.F. Smith and J.D. Lewin, Phys. Rep. 187, 203 (1990).
- [17] L. Baudis et al., NIMA 418/2-3 348-354 (1998).
- [18] D. Reusser et al., Phys. Lett. B 255, (1991) 143
- [19] P. Belli et al., in Proc. of the Second Int. Conference on Dark Matter in Astro- and Particle Physics (DARK98) July 1998, Heidelberg, Eds. H.V. Klapdor-Kleingrothaus and L. Baudis, IOP, Bristol& Philadelphia, 1999, p. 711.
- [20] R. Abusaidi et al., CDMS Collaboration, Phys.Rev.Lett. 84 (2000) 5699-5703
- [21] M. Bravin et al., Astrop. Physics 12 (1999) 107.
- [22] R.W. Schnee et al., in Proc. of the Third Int. Symposium on Sources and detection of dark matter in the Universe, February 1998, Marina del Rey, Editor D.B. Cline, Physics Reports 307 (1998), p. 283.
- [23] R. Bernabei et al., Phys. Lett. B 424 (1998) 195, Phys. Lett. B 450 (1999) 448, INFN/AE-00/01, February 2000.
- [24] V.A. Bednyakov and H.V. Klapdor-Kleingrothaus, Phys. Rev. D 62 (2000) 043524
- [25] J. Hellmig, Diploma Thesis, University of Heidelberg 1995
- [26] F. Schwamm, Diploma Thesis, University of Heidelberg 1999

TABLE I. Detector properties for the small inner Ge-detector and the active veto-shield, the outer well-type Ge-detector.

Property	Inner Detector	Outer Detector
Crystal Type	p-type	n-type
Mass [g]	202	2111
Active Volume [cc]	37	383
Crystal diameter [mm]	35.2	84.4
Crystal length [mm]	40.3	86.2
Operation Bias	+2500	-1500
FWHM (1332 keV) [keV] (ORTEC)	1.92	4.41
FWHM (1332 keV) [keV] (Heidelberg)	1.87	4.45
Threshold Heidelberg [keV]	2.5	7.5
Optimum pulse shaping [μ s]	4	2-3

TABLE II. Electronic energy thresholds and zero energy resolutions for the inner and outer Ge-detector.

	threshold [keV]	$\sigma_0 = \text{FWHM}_0/2.35$
inner	2.0	0.40
outer	7.5	1.42

TABLE III. Number of counts per 1 keV energy bin after an exposure of 9.9 kg d.

Bin [keV]	Counts/keV	Bin [keV]	Counts/keV
2-3	1	25-26	1
3-4	2	26-27	1
4-5	7	28-29	3
5-6	6	29-30	0
6-7	11	30-31	0
7-8	8	31-32	0
8-9	12	32-33	1
9-10	38	33-34	3
10-11	37	34-35	4
11-12	1	35-36	4
12-13	1	36-37	1
13-14	1	37-38	1
14-15	2	38-39	3
15-16	1	39-40	2
16-17	0	40-41	1
17-18	1	41-42	0
18-19	0	42-43	2
19-20	3	43-44	1
20-21	1	44-45	0
21-22	0	45-46	0
22-23	0	46-47	1
23-24	0	47-48	0
24-25	1	48-49	2

TABLE IV. List of parameters used for calculating WIMP spectra.

Parameter	Value
WIMP velocity distribution	270 km/s
Escape velocity	580 km/s
Earth velocity	245 km/s
WIMP local density	0.3 GeV/cm ³
natural Ge mass	72.61 g/mol

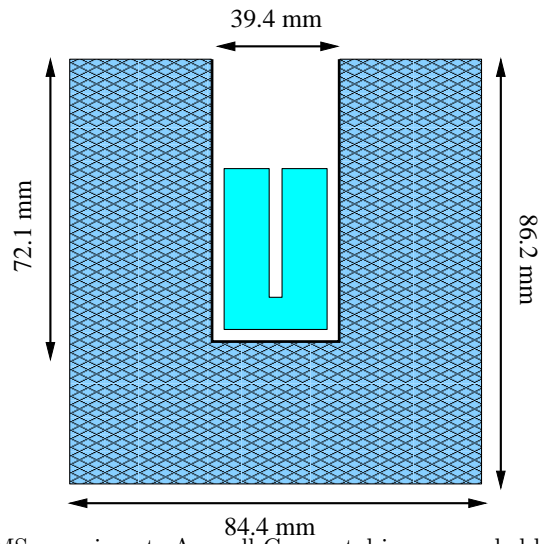


FIG. 1. Schematic view of the HDMS experiment. A small Ge-crystal is surrounded by a well type Ge-crystal, the anticoincidence between them is used to suppress the background created by external photons.

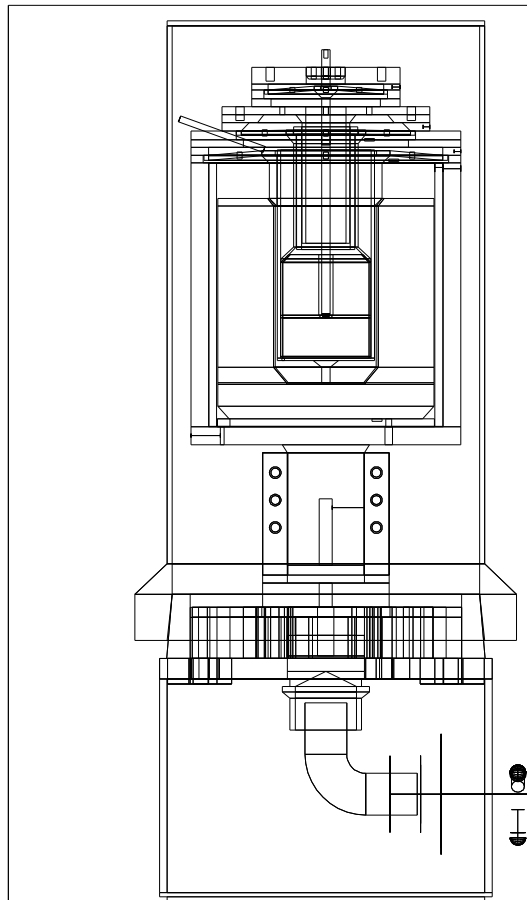


FIG. 2. Detailed view of the inner and outer Germanium crystals in their copper holder system.

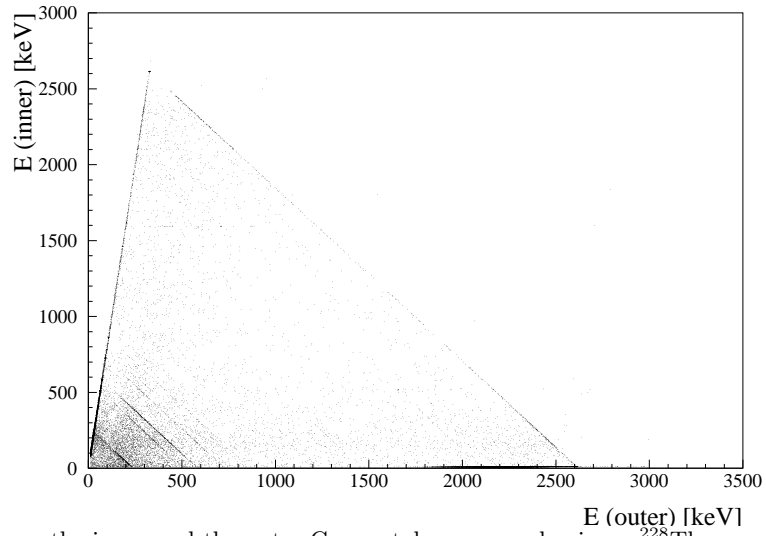


FIG. 3. Cross-talk between the inner and the outer Ge crystals, measured using a ^{228}Th source. The linear correlations are corrected off-line in order to obtain the true anticoincidence spectra.



FIG. 4. The HDMS detector in its open shield during the installation in the Gran Sasso Underground Laboratory. The inner shield is made of 10 cm of electrolytic copper, the outer one of 20 cm of Boliden lead.

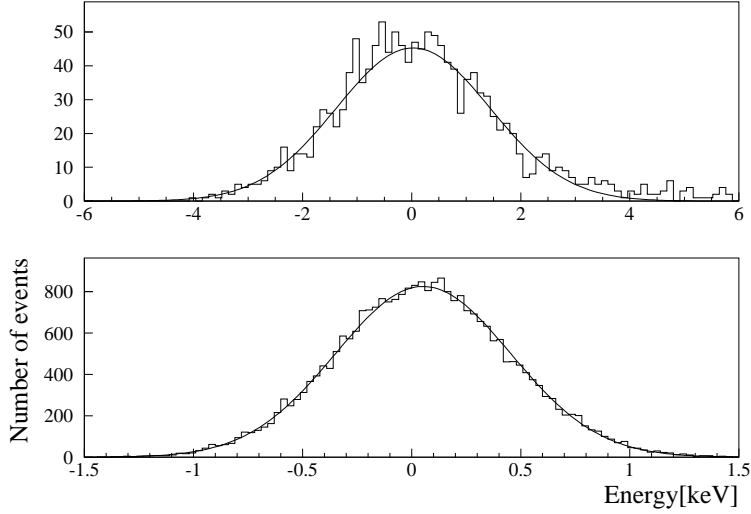


FIG. 5. Zero energy resolution of the outer (upper) and inner (lower) detector, determined from the cross-talk correction. The widths of the Gauss-curves are 1.42 keV and 0.4 keV, respectively.

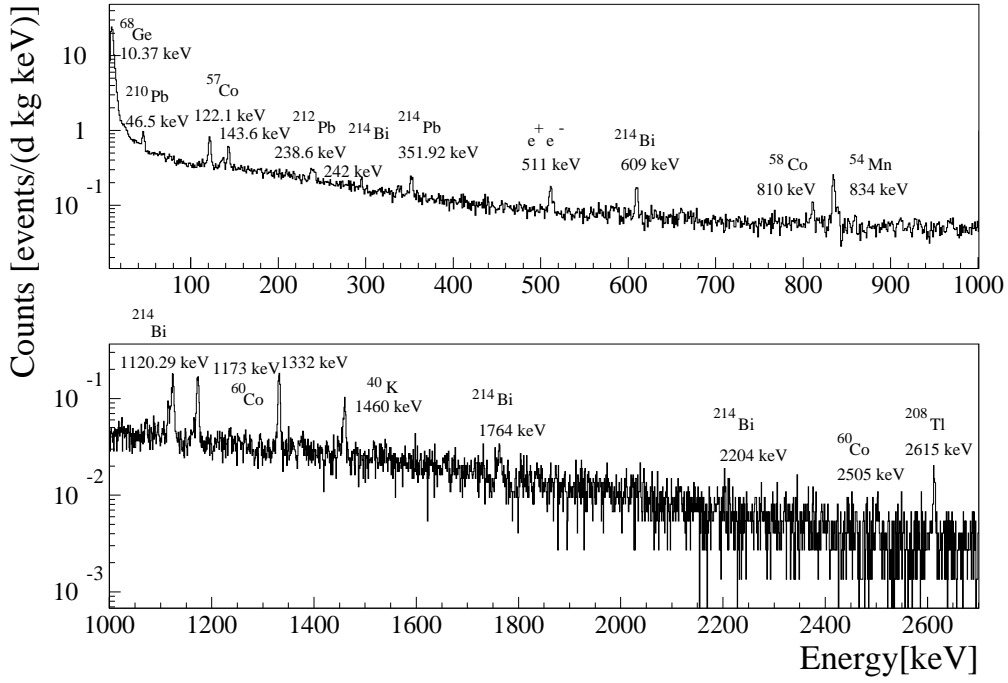


FIG. 6. Sum spectrum of the outer detector after 363 raw live-days of data taking. The most prominent lines are labeled.

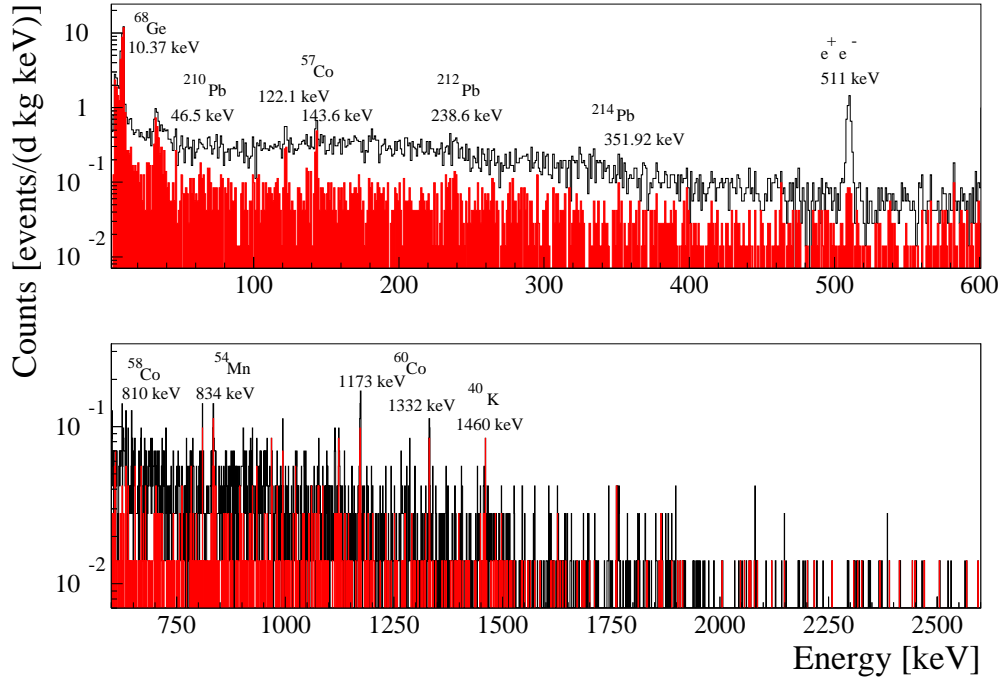


FIG. 7. Sum spectrum of the inner detector after 363 raw live-days of data taking. The most prominent lines are labeled. The filled histogram is the resulting spectrum after computing the anticoincidence with the outer detector.

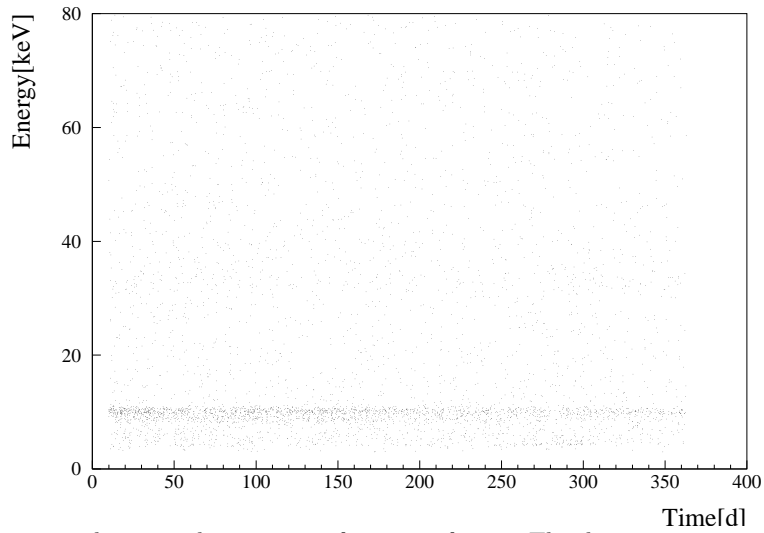


FIG. 8. Energy depositions in the inner detector as a function of time. The decreasing activity of ^{68}Ge is nicely visualized. No microphony (bursts) beyond 2 keV can be seen.

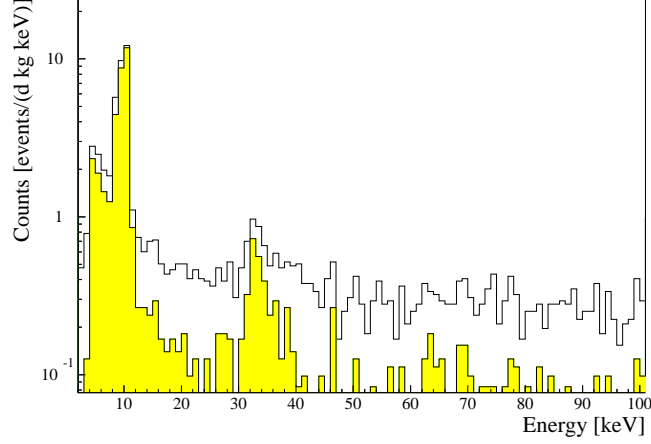


FIG. 9. Low energy spectrum of the inner, natural Ge detector before and after (filled histogram) the anticoincidence is applied with the outer Ge detector. The internal, low energy X-rays, as well as the structure centred at 32 keV are not removed by the anticoincidence with the outer detector. A ${}^3\text{H}$ β^- -spectrum with endpoint at 18 keV is most likely present.

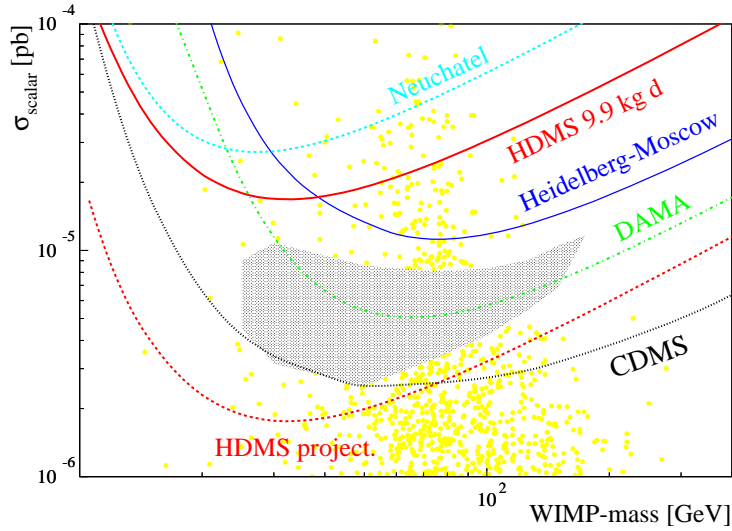


FIG. 10. WIMP-nucleon cross section limits as a function of the WIMP mass for spin-independent interactions. Solid thick line: 90% C.L. limit of the HDMS prototype with 9.9 kg d exposure. Solid thin line: limit of the Heidelberg-Moscow experiment [7], light dashed line: Ge limit from Neuchâtel [18], dashed-dotted line: DAMA limit [19], dotted line: CDMS 2000 limit [20]. The dark dashed curve is the expectation for HDMS with a background index of 0.07 events/kg d keV in the 2-30 keV energy region. The filled contour represents the 2σ evidence region of the DAMA experiment [23]. The experimental limits are compared to expectations (scatter plot) for WIMP-neutralinos calculated in the MSSM parameter space at the weak scale (without any GUT constraints) under the assumption that all superpartner masses are lower than 300 GeV - 400 GeV [24].